Structure, Vol. 13, 591–600, April, 2005, ©2005 Elsevier Ltd All rights reserved. DOI 10.1016/j.str.2004.12.019

A Gate in the Selectivity Filter of Potassium Channels

Simon Bernèche[1,2,*] and Benoît Roux[1]
[1]Department of Physiology and Biophysics
Weill Medical College of Cornell University
1300 York Avenue
New York, New York 10021

Summary

The selectivity filter of potassium channels is the structural element directly responsible for the selective and rapid conduction of K^+, whereas other parts of the protein are thought to function as a molecular gate that either permits or blocks the passage of ions. However, whether the selectivity filter itself also possesses the ability to play the role of a gate is an unresolved question. Using free energy molecular dynamics simulations, it is shown that the reorientation of two peptide linkages in the selectivity filter of the KcsA K^+ channel can lead to a stable nonconducting conformational state. Two microscopic factors influence the transition toward such a conformational state: the occupancy of one specific cation binding site in the selectivity filter (S_2), and the strength of intersubunit interactions involving the GYG signature sequence. These results suggest that such conformational transitions occurring in the selectivity filter might be related to different K^+ channel gating events, including C-type (slow) inactivation.

Introduction

In excitable tissue, the normal propagation of electric signals (action potentials) requires a tight control of ion conduction through selective channels (Hille, 1992). Triggered by the cell membrane depolarization, different types of potassium channels open their pore, allowing K^+ ions to diffuse down their electrochemical gradient toward the extracellular space and repolarize the cell to negative potential. Recent progress in the structural characterization of K^+ channels helps elucidate several of their most important functional features in molecular terms (Doyle et al., 1998; Yellen, 1998; Zhou et al., 2001). Different parts of the channel protein play clear and distinct functional roles. The narrowest part of the pore—the selectivity filter—allows the rapid and selective conduction of K^+ ions (Doyle et al., 1998; Bernèche and Roux, 2001, 2003; Morais-Cabral et al., 2001; Zhou et al., 2001), while the last helical segment of each of the four subunits forms a bundle crossing that constitutes an intracellular gate regulating access to the pore (Perozo et al., 1999; Roux et al., 2000; del Camino and Yellen, 2001; Jiang et al., 2002; Soler-Llavina et al., 2003). The crystallographic structure of the MthK channel, in which the inner helices are sharply bent at a conserved glycine residue acting as a hinge (Jiang et al., 2002), presents a general paradigm for such a gating mechanism. Although this is less well understood, several lines of evidence suggest that the opening and closing of K^+ channels may implicate the selectivity filter itself (i.e., that the selectivity filter might have the ability to act as a gate by switching between conducting and nonconducting states).

The possibility that the selectivity filter of K^+ channels could act as a gate bears considerably on our understanding of a wide range of observed phenomenon. In particular, a subtle conformational change of the selectivity filter has been implicated in C-type (slow) inactivation (Lopez-Barneo and Aldrich, 1993; Liu et al., 1996; Starkus et al., 1997), one of the mechanisms by which voltage-gated (Kv) channels spontaneously stop conducting K^+ ions (Yellen, 1998). Furthermore, a fast gating mechanism associated with the selectivity filter, which manifests itself as rapid opening and closing events in single channel recordings (channel flickerings), is thought to play an important role in the regulation of inward rectifier K^+ (Kir) channels (Bichet et al., 2003). There is also some evidence that the selectivity filter of the KcsA channel can act as a gate. For example, the probability of the open state increases significantly when Rb^+ rather than K^+ is used as the permeant ion (LeMasurier et al., 2001), suggesting that the ion present in the narrow pore ion is affecting some local process rather than a MthK-like intracellular gating mechanism occurring tens of angstroms away.

Computational studies show that ion movement through the channel takes place in a highly concerted way, as the K^+ in the pore undergo sudden hopping transitions between stable multi-ion configurations (Bernèche and Roux, 2001, 2003), consistent with diffraction data (Morais-Cabral et al., 2001; Zhou et al., 2001). While the repulsion between the cations is needed for rapid conduction (Bernèche and Roux, 2001), their presence contributes to the overall stability of the structure by counterbalancing the repulsive forces between the negatively charged oxygen atoms of the backbone carbonyls (Loboda et al., 2001). The selectivity filter was seen to distort considerably during molecular dynamics (MD) simulations of the KcsA K^+ channel carried out in the absence of ions in the pore (Shrivastava and Sansom, 2000). Additional information about the ability of the selectivity filter to distort is provided by a crystallographic X-ray structure of KcsA determined at low K^+ concentration (Zhou et al., 2001). In this structure, the orientation of the carbonyl group of Val76 is significantly tilted relative to the structure determined at high K^+ concentration. The structural variability of this region of the pore had also been noted previously, as spontaneous reorientation transitions of the Val76-Gly77 peptide linkage were observed previously in molecular dynamics (MD) simulations of the KcsA channel (Bernèche and Roux, 2000). This conformational transition is illustrated in Figures 1C and 1D and is described in further detail below. Similar reorientation transitions have also been observed in several

*Correspondence: simon.berneche@unibas.ch
[2]Present address: Biozentrum, University of Basel, 4056 Basel, Switzerland.

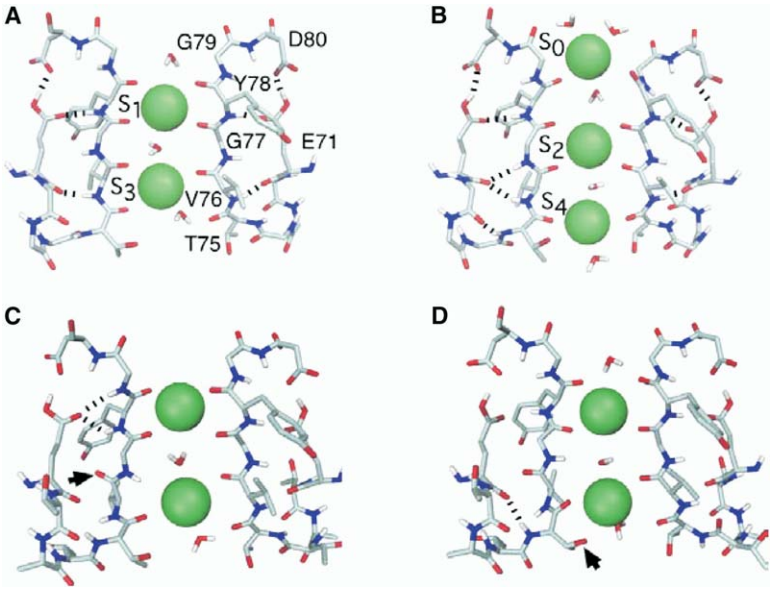

Figure 1. Details of the Selectivity Filter of the KcsA K^+ Channel

For clarity, only two of the four subunits are shown and some side chains are omitted. The dashed lines highlight the hydrogen bonds stabilizing the selectivity filter. Results from both X-ray crystallography (Morais-Cabral et al., 2001; Zhou et al., 2001) and molecular dynamics (MD) free energy simulations (Aqvist and Luzhvov, 2000; Bernèche and Roux, 2001) show that five specific cation binding sites, hereafter referred to as S_0 to S_4, are disposed along the narrow pore of the KcsA K^+ channel. The figures in (A) and (B) correspond to the two main intermediate states that enable fast ion conduction with K^+ in sites S_1 and S_3 (A) and in sites S_2 and S_4 (B). The latter configuration is enforced by the presence of a third cation, K^+ or tetraethylammonium (TEA), in the binding site S_0 located at the extracellular end of the selectivity filter (Bernèche and Roux, 2001; Crouzy et al., 2001; Zhou et al., 2001; Thompson and Begenisich, 2003). The figures in (C) and (D) illustrate the conformational transition of the selectivity filter as observed in Bernèche and Roux (2000). The complete transition takes place in two steps, respectively involving the Val76-Gly77 (C) and Thr75-Val76 (D) amide planes in one of the four monomers. (C) In a first step, the carbonyl group of Val76 points away from the pore (indicated by an arrow). (D) In a second step, the carbonyl and side chain hydroxyl group (indicated by an arrow) of Thr75 closely coordinate the ion in S_3, while the amide group forms a strong hydrogen bond with the carbonyl group of Glu71 (dashed line). All molecular pictures were drawn with DINO (http://www.dino3d.org).

independent MD studies of KcsA based on different force fields and simulation methodologies (Allen et al., 2000; Bernèche and Roux, 2000; Guidoni et al., 2000; Shrivastava et al., 2002; J. Åqvist, personal communication), as well as in simulations of Kir6.2 (Capener et al., 2003) and kirBAC (Domene et al., 2004). The conformational states observed in MD and X-ray are not identical. In the low-K^+ X-ray structure determined with 2 mM KCl and 148 mM NaCl (PDB ID 1K4D), the Val76 amide plane of the four subunits is tilted simultaneously by about 45° in a 4-fold symmetric manner, and the selectivity filter remains in the vicinity of the structure determined with 150 mM KCl (PDB ID 1K4C) (Zhou et al., 2001) (see the Supplemental Data available with this article online). In the configuration observed in MD trajectories the amide plane of a single one of the four subunits is flipped by about 180°, breaking the 4-fold symmetry (Bernèche and Roux, 2000). The observed structural flexibility of the backbone of the selectivity filter is consistent with the presence of glycine residues. Those are absolutely required for folding the TVGYG signature sequence into the ion-conducting conformation, with all backbone carbonyl oxygen atoms oriented toward the central pore axis (Figures 1A and 1B). In particular, the dynamical transition observed in the MD trajectory (Bernèche and Roux, 2000) converts Gly77 of one subunit from a right-handed backbone conformation easily accessible to glycines to a left-handed one accessible to all amino acids (see Supplemental Data). This strongly suggests that the important backbone flexibility of the selectivity filter conferred by the glycine residues and the existence of conformational states of broken symmetry may be a genuine property of the selectivity filter of K^+ channels.

These observations provide us with an opportunity to address questions about the ability of the selectivity filter to adopt nonconducting states and, thus, act as a gate. To characterize the conduction of K^+ through the selectivity filter in the conformation of broken symmetry, a multi-ion free energy surface using umbrella sampling MD simulations is calculated. The result shows that the K^+ current should indeed be significantly reduced when the selectivity filter adopts this conformation. To further understand the significance of this result, the microscopic factors that influence the dynamic stability of the selectivity filter are examined by calculating the free energy profiles governing the transition between the conducting and nonconducting conformational states. It is found that this transition depends on the K^+ occupancy of one specific cation binding site in the selectivity filter (S_2) and on the strength of intersubunit interactions, particularly those implicating the highly conserved aromatic residue in the GYG signature sequence. The results are discussed in the light of the various experimental observations on K^+ channels and suggest that such conformational transitions occurring in the selectivity filter might be related to different K^+ channels gating events.

Results

A Conformational State of Broken Symmetry

The complete transition leading to the stable isomerized conformation shown in Figure 1D takes place in two steps, respectively involving the Val76-Gly77 and Thr75-Val76 peptide linkages in one of the four monomers (Bernèche and Roux, 2000). In the initial step, the amide plane Val76-Gly77 undergoes a 180° reorientation, flipping the backbone carbonyl oxygen of Val76 away from the conduction pathway (Figure 1C). The

180° reorientation of the Val76-Gly77 peptide linkage (required to initiate the complete transition to the nonconducting state) is not energetically prohibitive because it is not strongly constrained by hydrogen bonding in the 4-fold symmetric conducting state (see Figures 1A and 1B); essentially, two backbone amides donors (Val76 and Gly77) share the same backbone carbonyl acceptor (Glu71). The initial Val76-Gly77 transition leads to an intermediate state of marginal stability, as the amide plane can rapidly return to its initial orientation (Bernèche and Roux, 2000). However, once the initial reorientation of the amide plane has occurred, a second transition involving Thr75 may then take place toward a stable conformational state (Figure 1D). In this conformation, the carbonyl oxygen and the side chain of Thr75 coordinate the K^+ in site S_3 while the amide group of Thr75 forms a strong hydrogen bond with the carbonyl group of Glu71 (dashed line in Figure 1D), thereby "locking" the selectivity filter in a state breaking the 4-fold symmetry. Remarkably, the ion in site S_3 does not seem to be strongly affected by the symmetry-breaking conformational change; it remains well coordinated by seven or eight oxygen ligands, either from other carbonyl groups or water molecules. Nonetheless, as shown below the loss of a favorable interaction with a single backbone carbonyl (Val76) is sufficient to have a large impact on the free energy barrier opposing the translocation of K^+ from S_3 to S_2.

The Free Energy Surface Governing K^+ Conduction

Using free energy MD simulations based on the structure of the KcsA channel, it was shown previously that free energy barriers on the order of 2 kcal/mol are observed along the ion permeation pathway in the selectivity filter of K^+ channels, implying that the process of ion conduction is limited by diffusion (Bernèche and Roux, 2001). More specifically, ion flux calculations using the multi-ion free energy surface calculated from MD yielded a maximum channel conductance on the order of 400–500 ps (Bernèche and Roux, 2003). The excellent agreement with experimental measurements (LeMasurier et al., 2001) gives strong support to the conclusion that ion conduction proceeds mainly according to the sequence of states: [S_3, S_1] ↔ [Cavity, S_3, S_1] ↔ [S_4, S_2, S_0] ↔ [S_4, S_2] ↔ [S_3, S_1] (Bernèche and Roux, 2001, 2003). Two of these ion configurations in the symmetric fast-conducting conformation of the selectivity filter are illustrated in Figures 1A and 1B. For the present study, similar free energy simulations were carried out to examine the ion conduction properties of the stable conformational state of broken symmetry, which is shown in Figure 1D. The resulting potential of mean force (PMF) is presented in Figure 2 as a two-dimensional topographic map of the free energy landscape governing the ion conduction through the selectivity filter of the K^+ channel. The two-dimensional map corresponds to a projection of the full PMF $W(z_1,z_2,z_3)$. It is observed that a free energy barrier of 4 to 5 kcal/mol between the states [Cavity, S_3, S_1] and [S_4, S_2, S_0] opposes the concerted multi-ion transition that is essential for rapid ion conduction. In contrast, there was only a barrier of about 2 kcal/mol for this process in the PMF calculated on the basis of the ion-conducting conformation of the selectivity filter (Bernèche and Roux, 2001, 2003). The conformational change involving Val76 and Thr75 alters the geometry of the cation binding site S_3, resulting in a tight coordination scheme that effectively "traps" a K^+ at this position. The increase of 2 to 3 kcal/mol represents a reduction of the current by a factor of at least 100. Thus, the reorientation of the Val76 carbonyl followed by the rearrangement of the adjacent Thr75 residue has the ability to act as a gate that can effectively block the pore. The conformational change and the local reorganization of water molecules also have an impact on the selectivity of the cation binding sites in the selectivity filter. The excess free energy difference ($\Delta\Delta G$) for the alchemical transformation of a K^+ into a Na^+ was calculated for the S_2 and S_3 binding sites in both the conducting and the nonconducting states. In site S_2, the $\Delta\Delta G$ decreased from +6.6 kcal/mol for the conducting state to +3.2 kcal/mol for the nonconducting state. In site S_3, the

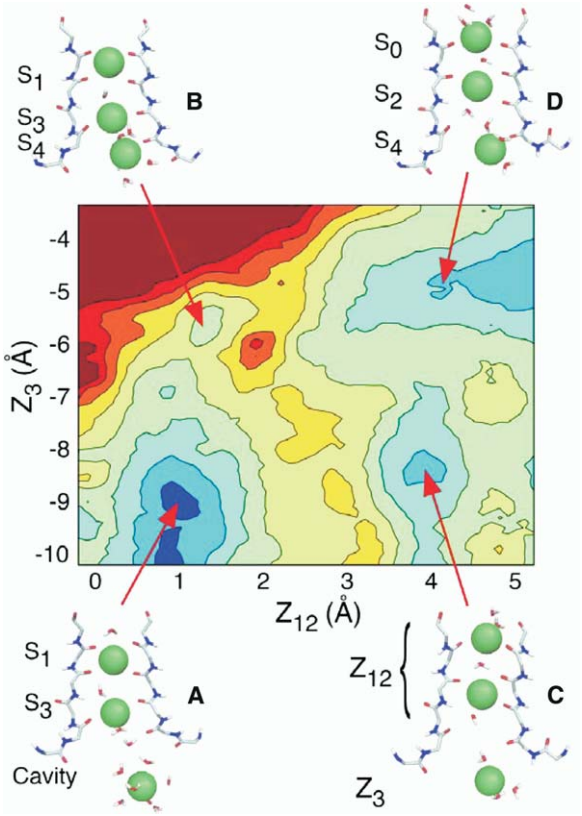

Figure 2. Topographic Free Energy Map of Ion Displacement in the Closed State of the Selectivity Filter Calculated from Umbrella Sampling MD Simulations

Each color level corresponds to 1 kcal/mol. The positions of the ions, Z_1, Z_2, and Z_3 (numbered in successive order starting from the outermost ion), are defined relative to the center-of-mass of the backbone atoms of residues Thr75-Val76-Gly77-Tyr78, which constitute the core of the KcsA selectivity filter. The definition of the reduced reaction coordinates (Z_{12}, Z_3) is indicated in (C), with Z_{12} corresponding to the center of mass of ions 1 and 2. The stable ion configurations are analogous to the ones found in the case of the conducting structure but the free energy barriers between them are larger.

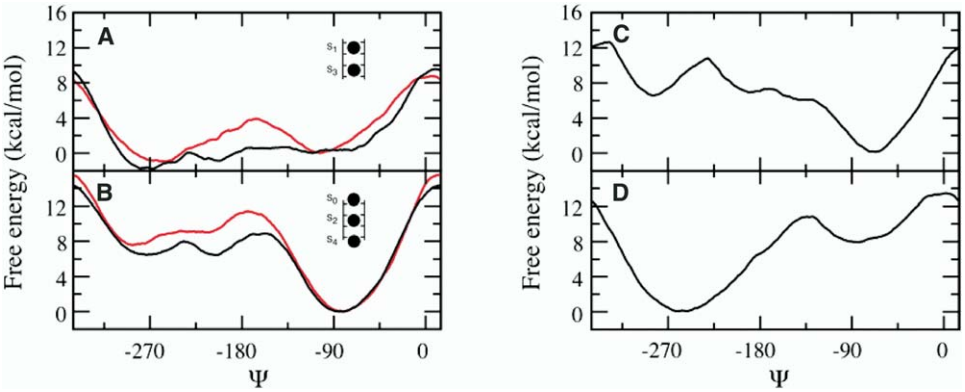

Figure 3. Microscopic Factors Affecting the Reorientation of the Val76-Gly77 Amide Plane

The total free energy is plotted as a function of the Ψ dihedral angle of Val76. (A) When ions occupy sites S_1 and S_3, a free energy barrier of 0.5 to 4 kcal/mol separates the conducting state (Ψ = −90°) from the conformation in which the Val76 carbonyl is flipped away from the pore (Ψ = −270°). (B) When sites S_0, S_2, and S_4 are occupied by K^+ ions, the barrier increases to values ranging from 9 to 12 kcal/mol. This important free energy barrier is mainly caused by the strong interaction between the Val76 carbonyls and the ion in site S_2. The red curves in (A) and (B) show that stabilization of the Tyr78-Trp68 intersubunit interactions leads to a free energy barrier increase of about 3 kcal/mol. (C) In the presence of ions in sites S_1 and S_3, a large free energy barrier prevents the reorientation of the amide plane if Gly77 is replaced by a D-Alanine. (D) Following the conformational change of Thr75, the Val76-Gly77 amide plane is locked around Ψ = −270° in a free energy well of about 11 kcal/mol, which stabilizes the nonconducting state of the selectivity filter.

ΔΔG decreased from +2.4 kcal/mol to about +0.4 kcal/mol. Although the specificity for K^+ over Na^+ is reduced in the state of broken symmetry, this is not associated with a physical constriction of the narrow pore according to the present computations. This observation is consistent with recent analysis showing that selectivity arises locally, from the electrostatic properties of the ligands coordinating the ion rather than from the sub-angtrom geometry of a rigid pore (Noskov et al., 2004).

Microscopic Factors Affecting the Transition to the Stable Nonconducting State

As described above, the complete transition toward the stable nonconducting conformational state of broken symmetry (Figure 1D) takes place in two sequential steps. The overall interconversion rates between the stable conducting and nonconducting states should be dominated by any slow process encountered during the complete conformational transition. In particular, microscopic factors that significantly increase the activation energy barrier for the reorientation of the peptide linkage Val76-Gly77 by 180° (Figure 1C) are preventing the initiation of a transition toward the nonconducting state and, thereby, are expected to increase the lifetime of the conducting state. It is, therefore, of interest to assess the microscopic factors influencing this initial step. To this end, we calculated the free energy profile as a function of the ψ dihedral angle of Val76 under various conditions. The results are shown in Figure 3. We first consider a channel occupied by K^+ in sites S_1 and S_3, as illustrated in Figure 1A. The free energy profile, presented in Figure 3A (black line), displays a barrier of about 0.5 kcal/mol between the ion-conducting state (ψ = −90°) and the intermediate state (ψ = −270°). In contrast, as shown in Figure 3B, the free energy barrier increases to about 9 kcal/mol if the sites S_0, S_2, and S_4 are occupied by K^+ (see Figure 1B). The large barrier preventing the reorientation of the Val76-Gly77 amide plane is due to the specific geometry of the S_2 binding site, in which a K^+ is tightly coordinated by eight carbonyl oxygen atoms (in comparison, a K^+ in S_3 is coordinated by five or six carbonyl oxygen atoms) (Bernèche and Roux, 2000). Interestingly, S_2 is the most selective of the five cation binding sites according to previous free energy calculations performed on the ion-conducting state (Aqvist and Luzhvov, 2000; Noskov et al., 2004).

The reorientation of the Val76 carbonyl group cannot take place simultaneously in more than a single subunit. Attempts to reorient a second Val76-Gly77 amide plane give rise to large free energy barriers or excessive deformations of the selectivity filter structure, which indicates that the state of broken symmetry is very stable. The presence of glycine residues in the GYG signature sequence is clearly required to initiate the conformational transition. As shown in Figure 3C, a large free energy barrier of more than 10 kcal/mol prevents the reorientation of the amide plane if Gly77 is substituted by a right-handed alanine (D-alanine), thus decreasing the probability of a transition toward the nonconducting state of the selectivity filter. Conversely, introduction of a small methyl group at position 77 does not perturb the symmetric ion-conducting conformation of the selectivity filter; the RMS deviation relative to the symmetric X-ray structure (1K4C) is essentially negligible. This result suggests that replacing the first glycine residue in the GYG signature sequence of K^+ channels by an unnatural D-alanine should increase the stability of the conducting state of the selectivity filter.

The second step, which leads to the stable nonconducting conformational state, involves the reorientation of the backbone and side chain of Thr75. During this transition, the backbone hydrogen bond between Glu71 and Val76 residues is replaced by a hydrogen bond between residues Glu71 and Thr75, resulting in a

tight coordination of the K^+ in S_3 (see Figure 1D). The conformational stability of the nonconducting state was assessed by calculating the PMF of the backbone dihedral angle of the Val76-Gly77 amide plane; the structure shown in Figure 1D was used as a starting point. Figure 3D shows that the Val76-Gly77 amide plane with its carbonyl group pointing away from the pore ($\psi = -270°$) is now trapped in a free energy well of about 11 kcal/mol, suggesting that the final nonconducting conformational state is very stable. Its lifetime of the state can be estimated directly from Kramer's transition rates using the calculated PMF for the backbone dihedral angle (see Experimental Procedures). The estimated transition rate from the nonconducting to the conducting state is $7.1 \times 10^3\ s^{-1}$, corresponding to a lifetime approaching the millisecond timescale (0.14 ms).

At any given instant during MD trajectories, the tetrameric channel does not present a perfect 4-fold symmetry because of thermal fluctuations (Bernèche and Roux, 2000); the symmetry is only recovered when properties averaged over a long time are considered. However, long-lived deviations from perfect 4-fold symmetry have an important impact on the free energy barrier opposing the reorientation of the carbonyl group of the Val76-Gly77 amide plane. The PMF shown in Figure 3 were calculated for a subunit that had undergone a transition of the selectivity filter in a previous simulation (Bernèche and Roux, 2000). The same PMF calculated by reorienting the carbonyl Val76 of other subunits yielded free energy barriers of 3.5 to 4 kcal/mol. Such differences, which certainly reflect an incomplete sampling, indicate that some additional slow intramolecular processes taking place on a timescale of several nanoseconds are playing a role. Further analysis indicated that the variability in the PMF is strongly correlated with the strength of an intersubunit hydrogen bond important for the stability of the selectivity filter involving Tyr78 and Trp68. During unbiased MD simulations, the Tyr78-Trp68 donor-acceptor distance fluctuates from 3 to 6 Å (Bernèche and Roux, 2000). Analysis of time series suggests that the probability of a reorientation of the Val76-Gly77 amide plane is reduced when the side chain of the adjacent Tyr78 is implicated in a strong hydrogen bond. How these complex interactions affect the structural flexibility and stability of the selectivity filter is, however, difficult to assess quantitatively. The barrier opposing the conformational change of the Val76-Gly77 amide plane could depend on the fluctuations of the Tyr78 side chain, which would be stabilized by its interaction with Trp68, or more generally, it might depend on the overall packing between the four subunits, which would be favored by stable Tyr78-Trp68 intersubunit interactions.

To assess the importance of these intersubunit interactions, the channel was simulated in the presence of energy restraints to stabilize the intersubunit hydrogen bonds between Tyr78 and Trp68 of all four subunits, imposing a donor-acceptor distance around 3.5 Å. The PMF corresponding to the reorientation of Val76 were then recalculated (the restraints were not applied during the PMF calculations). Following the imposed stabilization of the Tyr78-Trp68 hydrogen bonds according to this procedure, the free energy barrier increased from 0.5 to 4 kcal/mol with K^+ in sites S_1 and S_3 (Figure 3A), and from 9 to 12 kcal/mol in the presence of an ion in site S_2 (Figure 3B). Stabilization of the Asp80-Arg89 intersubunit salt bridges according to the same procedure had similar, though smaller, effects on the reorientation of Val76. Interestingly, a given hydrogen bond between Tyr78-Trp68 does not have a simple effect within a single subunit. Test calculations with distance restraints applied to only three of the four Tyr78-Trp68 hydrogen bonds (excluding the Tyr78 of the subunit for which the PMF calculation was done) showed qualitatively the same results, suggesting that the four subunits interact cooperatively to stabilize the selectivity filter in the ion-conducting conformation.

Discussion

The central result of the present study is the characterization of the multi-ion free energy surface governing ion conduction through the selectivity filter in the stable state of broken symmetry shown in Figure 1D. The multi-ion PMF (Figure 2) shows that the free energy barriers opposing K^+ translocation have increased significantly, by roughly 2–3 kcal/mol, yielding a channel conductance reduced by a factor of ~100. Essentially, such a conformational state of the selectivity filter can be considered as nonconducting or blocked. It would also be of interest to assess also the ion-conducting properties of other conformation of the selectivity filter, e.g., the 4-fold symmetric X-ray structure determined at 2 mM KCl and 148 mM NaCl (PDB ID 1K4D) (Zhou et al., 2001), although the likelihood that some Na^+ ions may occupy the selectivity filter under these conditions implies that such a calculation should take into account all possible permutation of K^+ and Na^+. Without further information about pore occupancy, this calculation becomes prohibitively difficult.

The nonconducting state of broken symmetry is very stable compared to the timescale of ion conduction. The return of the selectivity filter to the conducting state is opposed by an activation free energy barrier of ~11 kcal/mol (see Figure 3D). An estimate based on Kramer's rate theory (see Experimental Procedures) indicates that the lifetime of the nonconducting state is 0.14 ms, i.e., comparable to the lifetime of fast gating events observed in single channel bilayer experiments with KcsA (LeMasurier et al., 2001). Gating kinetic events on a similar time scale are also observed for Kv and Kir channels (Bichet et al., 2003; Schönherr and Heinemann, 1996; Smith et al., 1996; Spector et al., 1996). Further stabilization of the nonconducting state by as little as 3–4 kcal/mol with small additional structural rearrangements (e.g., one hydrogen bond) could increase the overall free energy barrier opposing the overall transition, resulting in a lifetime on the order of hundreds of milliseconds for the nonconducting state (see Figure 3D).

The complete transition from the conducting state to the nonconducting states takes place in two steps, an initial reorientation of the Val76-Gly77 peptide linkage followed by a rearrangement of the sidechain and backbone of Thr75. Any microscopic factors that significantly increase the activation energy barrier for this initiating process are expected to oppose transitions to-

ward the nonconducting state and therefore increase the lifetime of the conducting state. For the sake of simplicity, the PMF for the backbone dihedral ψ of Val76 was calculated with K^+ ions occupying different positions in the pore. Although a complete characterization of the coupling between ion translocation and the reorientation of the Val76-Gly77 peptide linkage using PMF calculations would be advantageous, such a computation would be quite challenging because of the high dimensionality of the process. The PMF calculations show that the free energy barrier opposing the initial step depends on interactions between the permeating ions and the backbone of the selectivity filter, as well as on interactions between the four subunits of the protein away from the conduction pore. The presence of a K^+ in the site S_2 appears to be particularly important, having the ability to completely prevent the initial conformational transition leading to the nonconducting state (Figure 3).

Conformational transitions to stable nonconducting states of the selectivity filter similar to the one characterized here could underlie a wide variety of phenomena displayed by K^+ channels. Depending on the molecular details of a given channel, such a process could conceivably also give rise to rapid "flickering current noise" (~1–10 milliseconds), blocks, or even inactivation (seconds). In the case of KcsA, our computations yield a channel blocked time of 0.14 ms. Transitions of the selectivity filter faster than ~10 microseconds would remain unresolved and appear as a reduction of the apparent channel conductance. At the moment the present work was going to press, an article describing ion permeation through the KcsA channel in which an unnatural D-alanine was introduced at the position of Gly77 was reported (Valiyaveetil et al., 2004). Although this report did not focus specifically on gating kinetics, the single channel recordings of the wild-type (Gly77) and modified (D-Ala77) channels shown in this paper are consistent with our predictions. The single channel traces of Figure 3 of Valiyaveetil et al. (2004) show that the ionic current through the wild-type channel (Figure 3A) is somewhat noisy, whereas the ionic current through the modified D-Ala77 KcsA (Figure 3B) channel is clean of such noise. As the single channel current traces were filtered at 500 Hz (Valiyaveetil et al., 2004), the additional noise is evidence for the presence of rapid channel block events on a millisecond timescale in KcsA with Gly77 relative to KcsA with D-Ala77, as predicted by the present computations (0.14 ms).

It is of interest to note that the present results bare some similarities with the factors that are known to affect one such phenomenon called C-type (slow) inactivation by which voltage-gated potassium (Kv) channels close their pore in response to prolonged cell depolarization. Although slow inactivation is often described in general terms as a "collapse of the pore," its underlying mechanism at the microscopic level has puzzled physiologists for more than a decade (Yellen, 1998). During C-type inactivation, Kv channels become transiently permeable for the smaller Na^+ ions (Starkus et al., 1997, 2000), a surprising observation that is commonly believed to imply a physical constriction of the pore followed by its collapse. According to the FEP calculations, there is a reduction of specificity K^+ over Na^+ in the state of broken symmetry. However, it should be noted that it is not caused by a physical constriction of the pore (see above). Various regions of the channel have been shown to have an impact on the rate of C-type inactivation, though there are indications from a number of experiments that some subtle structural rearrangements of the selectivity filter (Lopez-Barneo and Aldrich, 1993; Liu et al., 1996; Starkus et al., 1997), perhaps even limited to a single ion binding site (Molina et al., 1997; Ogielska and Aldrich, 1999), are implicated. It has been proposed on the basis of electrophysiological and mutagenesis experiments that the occupancy of a specific binding site along the ion permeation pathway prevents the development of C-type inactivation (Baukrowitz and Yellen, 1996; Molina et al., 1997; Kiss and Korn, 1998; Ogielska and Aldrich, 1999; Andalib et al., 2004), which is consistent with the present results. Furthermore, experimental results showing that the development of C-type inactivation arises from a cooperative mechanism involving the four subunits (Ogielska et al., 1995; Panyi et al., 1995) are broadly consistent with the sensitivity of the conformational transition on interactions between the subunits. This is also in broad agreement with the experimentally observed sensitivity of the conductance, mean open time, and selectivity of K^+ channels on single-point mutations affecting the intersubunit interactions near the selectivity filter (Chapman et al., 2001).

One of the hallmark functional signatures of C-type inactivation is its sensitivity to the concentration of extracellular cations. Notably, increase of the extracellular concentration of K^+ or tetraethylammonium (TEA^+) is known to decrease the rate of inactivation (Choi et al., 1991; Lopez-Barneo and Aldrich, 1993). At the microscopic level, this may be understood by considering the influence of extracellular cations on the stable multi-ion configurations observed in the selectivity filter. MD calculations have shown that extracellular K^+ and TEA^+ ions can bind to the site S_0 near the external mouth of the pore and, by doing so, stabilize K^+ ions in sites S_2 and S_4 (Bernèche and Roux, 2001, 2003; Crouzy et al., 2001); this prediction has been confirmed experimentally (Thompson and Begenisich, 2003). The presence of a cation in the extracellular binding site S_0 forces the occupancy of site S_2 by a K^+ (Figure 1B), thereby reducing the propensity of the selectivity filter to undergo a transition toward its nonconducting state (see Figure 4). Similarly, the present model might provide a rational basis to explain the observed influence of the transmembrane potential on C-type inactivation rate (Starkus et al., 2000; Klemic et al., 2001), as the applied voltage has a direct effect on the ion occupancy in the selectivity filter (see Figure 4). On a related aspect, it is well known that Kv channels need to be exposed to hyperpolarized transmembrane potentials to recover from inactivation. A mechanical coupling to the voltage sensor—the same that controls the activation gate—is usually proposed as the basis of this process (Olcese et al., 1997; Loots and Isacoff, 2000). Without excluding additional conformational changes involving the voltage sensor (Olcese et al., 1997), the present results suggest that voltage-induced displacement of K^+ from the state [S_3, S_1] to the state [S_4, S_2] might also play an important role in relieving channels

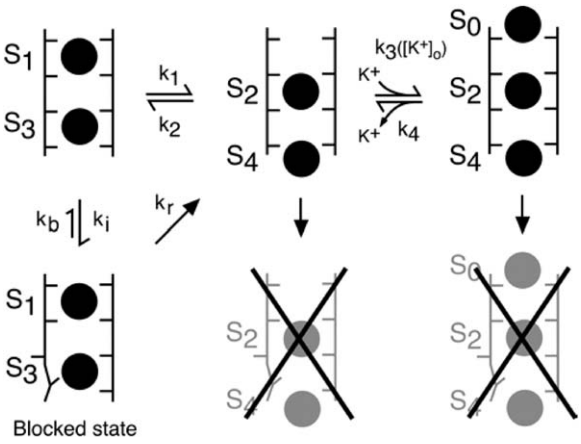

Figure 4. Schematic Diagram Summarizing the Coupling between Ion Occupancy and the Conformational Transition to the Nonconducting State

In the absence of transmembrane potential, the configurations S_1-S_3 and S_2-S_4 are in equilibrium ($k_1 = k_2$). Membrane depolarization (positive voltage shift) favors the state S_1-S_3, while membrane polarization (negative voltage shift) favors the state S_2-S_4. The top-right pictogram illustrates that the presence of an ion in site S_0 stabilizes the ions in the configuration S_2-S_4. Raising the extracellular K^+ concentration ($[K^+]_o$) favors the occupancy of site S_0 (k_3 increases with $[K^+]_o$) and, as a consequence, the occupancy of sites S_2 and S_4. Transition to a blocked or inactivated state is only possible from the top-left state in which site S_2 is not occupied. Speculatively, the transition corresponding to a voltage-dependent relief from inactivation is shown (k_r).

from inactivation by promoting the transition of the selectivity filter toward its ion-conducting conformation.

One structural determinant of the kinetics of C-type inactivation appears to be the presence of a hydrogen bond formed between the tyrosine from the GYG moiety and a tryptophan from an adjacent subunit, corresponding to Tyr78 and Trp68 in KcsA. Mutations of these residues (Heginbotham et al., 1994), or of surrounding residues (Lopez-Barneo and Aldrich, 1993; Perozo et al., 1993; Yang et al., 1997; Larsson and Elinder, 2000; Ortega-Sáenz et al., 2000), have important effects on the rate of C-type inactivation. In the hERG cardiac K^+ channel, the corresponding residues are replaced by two nonpolar Phe, which cannot form stabilizing hydrogen bonds. Consistent with the present analysis, hERG displays an extremely fast C-type inactivation, which gives rise to its physiologically important inward rectification property (Schönherr and Heinemann, 1996; Smith et al., 1996; Spector et al., 1996); the fast exit rate from its nonconducting inactivated state (milliseconds) is also functionally important. By opening its pore mainly at negative voltages, hERG plays a crucial role in the last phase of the repolarization of cardiac cells and sustains spike-frequency adaptation. The present model, which couples the rate of inactivation with the ion occupancy in the selectivity filter, suggests a simple molecular mechanism by means of which the conduction properties of hERG could vary with the extracellular K^+ concentration and the transmembrane potential (see Figure 4). Understanding the microscopic details of C-type inactivation and the inward rectification mechanism of hERG (I_{kr}) is important to elucidate the action mechanism of therapeutic agents such as use-dependent K^+-channel blockers, and could help to improve treatments of arrhythmia (Baukrowitz and Yellen, 1996; Smith et al., 1996).

Although the results and conclusions of the present computational study based on the bacterial KcsA channel are suggestive, they are necessarily incomplete. First, the present study is limited by the imperfections of the computational model. One particularly important source of uncertainty in the calculation is the difficulty of determining, from experiments or ab initio quantum mechanical calculations, the absolute magnitude of the energy barrier for backbone torsion angles (Feig et al., 2003). Thus, emphasis should be placed on the relative variations of the calculated free energy barriers, rather than on their absolute values. Furthermore, different factors in the computations that might have an impact on the stability of the selectivity filter are difficult to sample thoroughly. For example, the lipids packed around the channel could affect the cohesion of the tetrameric channel and, indirectly, the stability of the selectivity filter. In addition to the difficulties arising from the imperfections of the computational model, the present conclusions are further limited because the ability of the bacterial KcsA channel to reflect the wide range of complex gating properties observed in eukaryotic and mammalian channels is uncertain. Although most K^+ channels, particularly Kv channels, are subject to slow inactivation, the phenomenon has not been directly established in the case of the prokaryotic KcsA channel. Chimeras of Kv channels incorporating the pore domain of KcsA exhibit some characteristics of C-type inactivation gating (Lu et al., 2001b), supporting the idea that the underlying molecular mechanism of C-type inactivation might also be occurring in the pore of KcsA. Nevertheless, how the properties of KcsA relate to those of eukaryotic and mammalian channels is unknown, notably because their gating properties differ significantly on all timescales. Similar conformational states could be accessible for different K^+ channels, though with large variations in kinetics (Smith et al., 1996).

The uncertainties of the calculations and the difficulties associated with comparing a bacterial channel to eukaryotic channels notwithstanding, the following observations are unambiguous. (1) A relatively modest and local structural rearrangement involving the Val76-Gly77 peptide linkage can lead to a stable conformational state of broken symmetry of the selectivity filter that does not conduct K^+. (2) Transitions to this conformational state are inhibited by the presence of a K^+ in the binding site S_2. (3) Transitions to this state are also sensitive to cooperative intersubunit interactions and particularly to the hydrogen bonding involving the highly conserved aromatic residue in the GYG signature sequence.

Conclusions

The selectivity filter of the K^+ channel can undergo a transition involving two amide planes (Val76-Gly77 and Thr75-Val76 in KcsA). MD free energy PMF calculations

show that such a modest rearrangement leads to a stable nonconducting conformational state of the selectivity filter, which is then effectively acting as a gate. This structural rearrangement involves only one of the four subunits at a time, breaking the 4-fold symmetry of the tetrameric channel. The first step, which initiates the conformational transition toward the nonconducting state, is very sensitive to the configurations of the ion occupying the selectivity filter and on intersubunit interactions. This suggests that there should be common as well as specific gating features for different K^+ channels. Notably, the initial step appears to be prevented by the presence of a K^+ in the cation binding site S_2. The nature of the conformational change underlying the gating process by the selectivity filter, as well as the microscopic factors observed to have an impact on it, bears some similarity to C-type (slow) inactivation. Nonetheless, depending on the particular molecular details of a specific channel, it is conceivable that such conformational transitions in the selectivity filter could occur on a wide range of timescales. Therefore, on a speculative note, we would like to propose that the conformational transition described here might be one of the molecular mechanisms underlying a broad range of electrophysiological phenomena that are observed in single channel recordings and that define the specific function of a given channel. With the recent advances in direct protein synthesis (Lu et al., 2001a) and site-specific substitutions by unnatural amino acids (Valiyaveetil et al., 2002, 2004) as well as in spectroscopy of membrane proteins (Riek et al., 1999; Torres and Arkin, 2002), it will become possible to directly probe the dynamics of the selectivity filter of the KcsA channel and test this hypothesis experimentally.

Experimental Procedures

Simulation System and Parameters

All the simulations were carried out using the program CHARMM (Brooks et al., 1983). The total number of atoms in the simulation system is slightly above 40000 (KcsA with Glu71 in its protonated form, 112 DPPC, 6532 water molecules, 3 K^+ in the pore and 12 K^+ and 23 Cl^- in the bulk solution). The channel axis is oriented along the Z-axis and the center of the membrane is at $Z = 0$. The simulation methodology has been described previously (Bernèche and Roux, 2000). In brief, the electrostatic interactions were computed with no truncation using the particle mesh Ewald (PME) algorithm (Essmann et al., 1995). The trajectories were generated with a timestep of 2 fs at constant pressure (1 Atm) and temperature (315 K for the selectivity calculations and dihedral angle PMFs, 330 K for the ion displacement PMF) (Feller et al., 1995). The PARAM22 potential function for proteins (MacKerell et al., 1998) and lipids (Schlenkrich et al., 1996), and the TIP3 water potential (Jorgensen et al., 1983) were used. The Lennard-Jones (LJ) parameters of the K^+ and Na^+ ions were previously adjusted to yield the experimental free energy in liquid water (Beglov and Roux, 1994). In addition, the LJ parameters for the cation-carbonyl oxygen pairs were refined to yield solvation free energies in liquid N-methylacetamide identical to those in bulk water.

Free Energy Calculations

(1) For the ion displacement PMF calculations, a total of 154 independent simulations of 100 ps with a biasing harmonic potential centered on Z_{12}, and Z_3 (varying successively from 0.0 to 5.0 and –10.0 to –3.5 every 0.5 Å, see Figure 2) were generated with a force constant of 20 kcal/mol·Å^2. The center-of-mass biasing potential on Z_{12} was implemented using the MMFP option of CHARMM (Brooks et al., 1983). The initial structure for this calculation was taken from simulation C1-MD-315K in Bernèche and Roux (2000).

(2) For each PMF calculation describing the reorientation of the Val76-Gly77 amide plane, 73 independent simulations of 25 ps with a biasing harmonic potential centered on the Ψ dihedral angle of Val76 (varying from –345° to 15° by a step of 5°) were generated with a force constant of 100 kcal/mol·rad^2. The calculations were first applied to the structure resulting from the equilibration of the entire system (presented in Bernèche and Roux, 2000). This structure was then further equilibrated for 10 ps using a 5 kcal/mol·Å half-harmonic restraint on each of the Y78-W68 hydrogen bonds acting only when the donor-acceptor distance (d_{DA}) was greater than 3.5 Å; the PMF calculation was repeated on the resulting structure (without the restraints). All umbrella sampling simulations were unbiased using the weighted histogram analysis method (WHAM) (Kumar et al., 1992).

(3) For the selectivity calculations, each alchemical free energy difference between K^+ and Na^+ was obtained from forward and backward MD/FES trajectories generated with the thermodynamic coupling parameter method (Kollman, 1993) for a total of 440 ps. The total free energy difference was then calculated using WHAM (Kumar et al., 1992).

Transition Rate

The transition rate was estimated from the PMF on the dihedral angle of Val76 following the procedure described in Crouzy et al., 1994. Assuming the system to be in a high friction, large activation energy regime, the Kramer transition rate between two stable states is given approximately by the expression:

$$k = \frac{D(\Psi_b)}{2\pi k_B T}[-W''(\Psi_b)W''(\Psi_w)]^{1/2} e^{-\Delta W/k_B T},$$

where $D(\Psi_b)$ is the diffusion constant calculated at the top of the barrier, W'' is the second derivative of the PMF estimated (at the barrier Ψ_b and well Ψ_w) by harmonic fits, and ΔW is the height of the activation energy barrier for the transition. The diffusion constant at the top of the barrier was calculated from the velocity-velocity autocorrelation function using a formalism based on the generalized Langevin equation (see Crouzy et al., 1994).

Supplemental Data

Supplemental Data, including atomic coordinates of KcsA in its nonconducting conformational state, animation of the transition from the conducting to the nonconducting state, a Ramachandran plot of the Val76-Gly77 amide plane, and illustration of the hydrogen bonding network surrounding the selectivity filter, are available at http://www.structure.org/cgi/content/full/13/4/591/DC1/.

Acknowledgments

Useful discussions with Sergey Noskov are gratefully acknowledged. S.B. is grateful to L. Parent, R. Sauvé, and J.-Y. Lapointe from the Université de Montréal for their inspiring comments and teaching. This work was supported by the National Institute of Health. Several calculations were performed at the National Center for Supercomputing Applications (NCSA) of the University of Illinois at Urbana-Champaign.

Received: July 29, 2004
Revised: November 5, 2004
Accepted: December 2, 2004
Published: April 11, 2005

References

Allen, T.W., Bliznyuk, A., Rendell, A.P., Kuyucak, S., and Chung, S.H. (2000). Molecular dynamics study of the KcsA potassium channel. J. Chem. Phys. *77*, 2502–2516.

Andalib, P., Consiglio, J.F., Trapani, J.G., and Korn, S.J. (2004). The

external TEA binding site and C-type inactivation in voltage-gated potassium channels. Biophys. J. *87*, 3148–3161.

Aqvist, J., and Luzhvov, V. (2000). Ion permeation mechanism of the potassium channel. Nature *404*, 881–884.

Baukrowitz, T., and Yellen, G. (1996). Use-dependent blockers and exit rate of the last ion from the multi-ion pore of a K^+ channel. Science *271*, 653–656.

Beglov, D., and Roux, B. (1994). Finite representation of an infinite bulk system: solvent boundary potential for computer simulations. J. Chem. Phys. *100*, 9050–9063.

Bernèche, S., and Roux, B. (2000). Molecular dynamics of the KcsA K^+ channel in a bilayer membrane. Biophys. J. *78*, 2900–2917.

Bernèche, S., and Roux, B. (2001). Energetics of ion conduction through the K^+ channel. Nature *414*, 73–77.

Bernèche, S., and Roux, B. (2003). A microscopic view of ion conduction through the K^+ channel. Proc. Natl. Acad. Sci. USA *100*, 8644–8648.

Bichet, D., Haass, F.A., and Jan, L.Y. (2003). Merging functional studies with structures of inward-rectifier K(+) channels. Nat. Rev. Neurosci. *4*, 957–967.

Brooks, B.R., Bruccoleri, R.E., Olafson, B.D., States, D.J., Swaminathan, S., and Karplus, M. (1983). CHARMM: a program for macromolecular energy minimization and dynamics calculations. J. Comput. Chem. *4*, 187–217.

Capener, C.E., Proks, P., Ashcroft, F.M., and Sansom, M.S. (2003). Filter flexibility in a mammalian K channel: models and simulations of Kir6.2 mutants. Biophys J. *84*, 2345–2356.

Chapman, M.L., Krovetz, H.S., and VanDongen, A.M.J. (2001). GYGD pore motifs in neighbouring potassium channel subunits interact to determine ion selectivity. J. Physiol. *530*, 21–33.

Choi, K.L., Aldrich, R.W., and Yellen, G. (1991). Tetraethylammonium blockade distinguishes two inactivation mechanisms in voltage-activated channels. Proc. Natl. Acad. Sci. USA *88*, 5092–5095.

Crouzy, S., Woolf, T.B., and Roux, B. (1994). A molecular-dynamics study of gating in dioxolane-linked gramicidin-A channels. Biophys. J. *67*, 1370–1386.

Crouzy, S., Bernèche, S., and Roux, B. (2001). Extracellular blockade of K^+ channels by TEA: results from molecular dynamics simulations of the KcsA channel. J. Gen. Physiol. *118*, 207–217.

del Camino, D., and Yellen, G. (2001). Tight steric closure at the intracellular activation gate of a voltage-gated K+ channel. Neuron *32*, 649–656.

Domene, C., Grottesi, A., and Sansom, M.S. (2004). Filter flexibility and distortion in a bacterial inward rectifier K+ channel: simulation studies of KirBac1.1. Biophys. J. *87*, 256–267.

Doyle, D.A., Cabral, J.M., Pfuetzner, R.A., Kuo, A., Gulbis, J.M., Cohen, S.L., Chait, B.T., and MacKinnon, R. (1998). The structure of the potassium channel: molecular basis of K^+ conduction and selectivity. Science *280*, 69–77.

Essmann, U., Perera, L., Berkowitz, M.L., Darden, T., Lee, H., and Pedersen, L.G. (1995). A smooth particle mesh Ewald method. J. Chem. Phys. *103*, 8577–8593.

Feig, M., MacKerell, A.D., and Brooks, C.L. (2003). Force field influence on the observation of pi-helical protein structures in molecular dynamics simulations. J. Phys. Chem. B *107*, 2831–2836.

Feller, S.E., Zhang, Y.H., Pastor, R.W., and Brooks, B.R. (1995). Constant pressure molecular dynamics simulation - the Langevin piston method. J. Chem. Phys. *103*, 4613–4621.

Guidoni, L., Torre, V., and Carloni, P. (2000). Water and potassium dynamics inside the KcsA Kt channel. FEBS Letters *477*, 37–42.

Heginbotham, L., Lu, Z., Abramson, T., and MacKinnon, R. (1994). Mutations in the K^+ channel signature sequence. Biophys. J. *66*, 1061–1067.

Hille, B. (1992). Ionic Channels of Excitable Membranes, Second Edition (Sunderland, MA: Sinauer Associates Inc.).

Jiang, Y., Lee, A., Chen, J., Cadene, M., Chait, B.T., and MacKinnon, R. (2002). Crystal structure and mechanism of a calcium-gated potassium channel. Nature *417*, 515–522.

Jorgensen, W.L., Chandrasekhar, J., Madura, J.D., Impey, R.W., and Klein, M.L. (1983). Comparison of simple potential functions for simulating liquid water. J. Chem. Phys. *79*, 926–935.

Kiss, L., and Korn, S.J. (1998). Modulation of C-type inactivation by K^+ at the potassium channel selectivity filter. Biophys. J. *74*, 1840–1849.

Klemic, K.G., Kirsch, G.E., and Jones, S.W. (2001). U-type inactivation of Kv3.1 and Shaker potassium channels. Biophys. J. *81*, 814–826.

Kollman, P.A. (1993). Free energy calculations: applications to chemical and biochemical phenomena. Chem. Rev. *93*, 2395–2417.

Kumar, S., Bouzida, D., Swendsen, R.H., Kollman, P.A., and Rosenberg, J.M. (1992). The weighted histogram analysis method for free-energy calculations on biomolecules, I. The method. J. Comp. Chem. *13*, 1011–1021.

Larsson, H.P., and Elinder, F. (2000). A conserved glutamate is important for slow inactivation in K^+ channels. Neuron *27*, 573–583.

LeMasurier, M., Heginbotham, L., and Miller, C. (2001). KcsA: it's a potassium channel. J. Gen. Physiol. *118*, 303–314.

Liu, Y., Jurman, M.E., and Yellen, G. (1996). Dynamic rearrangement of the outer mouth of a K^+ channel during gating. Neuron *16*, 859–867.

Loboda, A., Melishchuk, A., and Armstrong, C. (2001). Dilated and defunct K channels in the absence of K^+. Biophys. J. *80*, 2704–2714.

Loots, E., and Isacoff, E.Y. (2000). Molecular coupling of S4 to a K^+ channel's slow inactivation gate. J. Gen. Physiol. *116*, 623–635.

Lopez-Barneo, J., and Aldrich, R.W. (1993). Effects of external cations and mutations in the pore region on C-type inactivation of Shaker potassium channels. Receptors Channels *1*, 61–71.

Lu, T., Ting, A.Y., Mainland, J., Jan, L.Y., Schultz, P.G., and Yang, J. (2001a). Probing ion pemeation and gating in a K^+ channel with backbone mutations in the selectivity filter. Nat. Neurosci. *4*, 239–246.

Lu, Z., Klem, A.M., and Yajamana, R. (2001b). Ion conduction pore is conserved among potassium channels. Nature *413*, 809–813.

MacKerell, A.D., Jr., et al. (1998). All-atom empirical potential for molecular modeling and dynamics studies of proteins. J. Phys. Chem. B *102*, 3586–3616.

Molina, A., Castellano, G., and López-Barneo, J. (1997). Pore mutations in Shaker K^+ channels distinguish between the sites of tetraethyllammonium blockade and C-type inactivation. J. Physiol. *499*, 361–367.

Morais-Cabral, J.H., Zhou, Y., and MacKinnon, R. (2001). Energetic optimization of ion conduction rate by the K^+ selectivity filter. Nature *414*, 37–42.

Noskov, S.Y., Bernèche, S., and Roux, B. (2004). Control of ion selectivity in potassium channels by electrostatic and dynamic properties of coordinating ligands. Nature *431*, 830–834.

Ogielska, E.M., Zagotta, W.N., Hoshi, T., Heinemann, S.H., Haab, J., and Aldrich, R.W. (1995). Cooperative subunit interactions in C-type inactivation of K channels. Biophys. J. *69*, 2449–2457.

Ogielska, E.M., and Aldrich, R.W. (1999). Functional consequences of a decreased potassium affinity in a potassium channel pore. J. Gen. Physiol. *113*, 347–358.

Olcese, R., Latorre, R., Toro, L., Bezanilla, F., and Stefani, E. (1997). Correlation between charge movement and ionic current during slow inactivation in Shaker K+ channels. J. Gen. Physiol. *11*, 579–589.

Ortega-Sáenz, P., Pardal, R., Castenallo, A., and López-Barneo, J. (2000). Collapse of conductance is prevented by a glutamate residue conserved in voltage-dependent K^+ channels. J. Gen. Physiol. *116*, 181–190.

Panyi, G., Sheng, Z., and Deutsch, C. (1995). C-type inactivation of a voltage-gated K+ channel occurs by a cooperative mechanism. Biophys. J. *69*, 896–903.

Perozo, E., MacKinnon, R., Bezanilla, F., and Stefani, E. (1993). Gat-

ing currents from a nonconducting mutant reveal open-closed conformations in Shaker K^+ channels. Neuron *11*, 353–358.

Perozo, E., Cortes, D.M., and Cuello, L.G. (1999). Structural rearrangements underlying K^+-channel activation gating. Science *285*, 73–78.

Riek, R., Wider, G., Pervushin, K., and Wuthrich, K. (1999). Polarization transfer by cross-correlated relaxation in solution NMR with very large molecules. Proc. Natl. Acad. Sci. USA *96*, 8–23.

Roux, B., Bernèche, S., and Im, W. (2000). Ion channel, permeation and electrostatics: insight into the function of KcsA. Biochem. *39*, 13295–13306.

Schlenkrich, M.J., Brickmann, J., MacKerell, A.D., Jr., and Karplus, M. (1996). An empirical potential energy function for phospholipids: criteria for parameter optimization and applications. In Biological Membranes. A Molecular Perspective from Computation and Experiment, K.M. Merz and B. Roux, eds. (Boston, MA: Birkhauser), pp. 31–81.

Schönherr, R.,, and Heinemann, S.H. (1996). Molecular determinant for activation and inactivation of HERG, a human inward rectifier potassium channel. J. Physiol. *39*, 635–642.

Shrivastava, I.H., and Sansom, M.S. (2000). Simulations of ion permeation through a potassium channel: molecular dynamics of KcsA in a phospholipid bilayer. Biophys. J. *78*, 557–570.

Shrivastava, I.H., Tieleman, D.P., Biggin, P.C., and Sansom, M.S.P. (2002). K^+ versus Na^+ ions in a K^+ channel selectivity filter: a simulation study. Biophys. J. *83*, 633–645.

Smith, P.L., Baukrowitz, T., and Yellen, G. (1996). The inward rectification mechanism of the HERG cardiac potassium channel. Nature *379*, 833–836.

Soler-Llavina, G.J., Holmgren, M., and Swartz, K.J. (2003). Defining the conductance of the closed state in a voltage-gated K channel. Neuron *38*, 61–67.

Spector, P.S., Curran, M.E., Zou, A., Keating, M.T., and Sanguinetti, M.C. (1996). Fast inactivation causes rectification of the I_{kr} channel. J. Gen. Physiol. *107*, 611–619.

Starkus, J.G., Kuschel, L., Rayner, M.D., and Heinemann, S.H. (1997). Ion conduction through C-type inactivated Shaker channels. J. Gen. Physiol. *110*, 539–550.

Starkus, J.G., Heinemann, S.H., and Rayner, M.D. (2000). Voltage dependence of slow inactivation in Shaker potassium channels – Results from changes in relative K^+ and Na^+ permeabilities. J. Gen. Physiol. *115*, 107–122.

Thompson, J., and Begenisich, T. (2003). External TEA block of shaker K channels is coupled to the movement of K^+ ions within the selectivity filter. J. Gen. Physiol. *122*, 239–246.

Torres, J., and Arkin, I.T. (2002). C-deuterated alanine: a new label to study membrane protein structure using site-specific infrared dichroism. Biophys. J. *82*, 1068–1075.

Valiyaveetil, F.I., MacKinnon, R., and Muir, T.W. (2002). Semisynthesis and folding of the potassium channel KcsA. J. Am. Chem. Soc. *124*, 9113–9120.

Valiyaveetil, F.I., Sekedat, M., Mackinnon, R., and Muir, T.W. (2004). Glycine as a D-amino acid surrogate in the K(+)-selectivity filter. Proc. Natl. Acad. Sci. USA *101*, 17045–17049.

Yang, Y., Yan, Y., and Sigworth, F.J. (1997). How does the W434F mutation block current in Shaker potassium channels? J. Gen. Physiol. *109*, 779–789.

Yellen, G. (1998). The moving parts of voltage-gated ion channels. Q. Rev. Biophys. *31*, 239–295.

Zhou, Y., Morais-Cabral, J.H., Kaufman, A., and MacKinnon, R. (2001). Chemistry of ion coordination and hydration revealed by a K^+ channel-Fab complex at 2.0 Å resolution. Nature *414*, 43–48.

Accession Numbers

The atomic coordinates of the nonconducting structure of the KcsA channel were deposited in the Protein Data Bank with ID code 1S33.